

Evaluating digital terrain indices for soil wetness mapping

A. M. Ågren et al.

Evaluating digital terrain indices for soil wetness mapping – a Swedish case study

A. M. Ågren¹, W. Lidberg¹, M. Strömngren², J. Ogilvie³, and P. A. Arp³

¹Dept. of Forest Ecology and Management, Swedish University of Agricultural Sciences, 901 83 Umeå, Sweden

²Dept. of Soil and Environment, Swedish university of Agricultural Sciences, P.O. Box 7014, 750 07 Uppsala, Sweden

³Forest Watershed Research Centre, Faculty of Forestry & Environmental Management, 28 Dineen Drive, UNB, Fredericton, NB E3B 583, Canada

Received: 24 February 2014 – Accepted: 21 March 2014 – Published: 11 April 2014

Correspondence to: A. M. Ågren (anneli.agren@slu.se)

Published by Copernicus Publications on behalf of the European Geosciences Union.

Title Page

Abstract

Introduction

Conclusions

References

Tables

Figures

◀

▶

◀

▶

Back

Close

Full Screen / Esc

Printer-friendly Version

Interactive Discussion



Abstract

Driving with forestry machines on wet soils within and near stream and lake buffers can cause soil disturbances, i.e. rutting and compaction. This – in turn – can lead to increased surface flow, thereby facilitating the leaking of unwanted substances into downstream environments. Wet soils in mires, near streams and lakes have particularly low bearing capacity and are more susceptible to rutting. It is important to model and map the extent of these areas and associated wetness variations. This can be done with adequate reliability using high resolution digital elevation model (DEM). In this article, we report on several digital terrain indices to predict soil wetness by wet-area locations. We varied the resolution of these indices to test what scale produces the best possible wet-areas mapping conformance. We found that topographic wetness index (TWI) and the newly developed cartographic depth-to-water index (D_{TW}) were the best soil wetness predictors. While the TWI derivations were sensitive to scale, the D_{TW} derivations were not and were therefore numerically fairly robust. Since the D_{TW} derivations vary by the area threshold used for setting stream flow initiation we found that the optimal threshold values varied by landform, e.g., 1–2 ha for till-derived landforms vs. 8–16 ha for a coarse-textured alluvial floodplain.

1 Introduction

It is well established that forestry, agriculture, transportation corridor (roads, trails), and other land-use practices can affect water quality (Buttle, 2011; Ahtiainen, 1992; Laudon et al., 2009; Schelker et al., 2012). One major threat for surface waters is soil erosion and subsequent increases in sediment loads. This, in turn, increases water turbidity and cover gravelly stream beds (Lisle, 1989), thereby decreasing the reproductive success of fresh-water fish (Burkhead and Jelks, 2001; Soulsby et al., 2001) and macro invertebrates (Lemly, 1982). In forestry, primary sediment sources are road crossings (Kreutzweiser and Capell, 2001), logging roads, skidder trails (Sidle et al., 2006), and

HESSD

11, 4103–4129, 2014

Evaluating digital terrain indices for soil wetness mapping

A. M. Ågren et al.

Title Page

Abstract

Introduction

Conclusions

References

Tables

Figures

◀

▶

◀

▶

Back

Close

Full Screen / Esc

Printer-friendly Version

Interactive Discussion



HESSD

11, 4103–4129, 2014

Evaluating digital terrain indices for soil wetness mapping

A. M. Ågren et al.

[Title Page](#)[Abstract](#)[Introduction](#)[Conclusions](#)[References](#)[Tables](#)[Figures](#)[⏪](#)[⏩](#)[◀](#)[▶](#)[Back](#)[Close](#)[Full Screen / Esc](#)[Printer-friendly Version](#)[Interactive Discussion](#)

ditching activities (Prevost et al., 1999). Rutting along slopes and wet soils can also affect water quality and aquatic habitat. For example, Munthe and Hultberg (2004) found that heavy forestry machinery traffic disturbs the soil, changes the water flow paths, and increases the local stream concentration of methylmercury (MeHg) with 600 % over a period of at least 3 years. Bishop et al. (2009) estimated that 9–23 % of the Hg in fish in Sweden is associated with the increased Hg outputs from clear-cutting. A study by Kronberg (2014) calculated that MeHg loads increased by 14 % after clear-cutting. To mitigate this effect, soil scarification and driving in wet and moist areas and across flow channels without brush mats should be avoided. Until now, areas that are sensitive to soil disturbances have not yet been mapped at resolutions sufficient to be included in forestry planning operations. Doing so, however, would greatly reduce environmentally and economically costly forest traffic “surprises”, and would be in compliance with a new policy from the Swedish forest industry suggesting that “driving on forest soils should be planned according to soil conditions, surface waters and cultural heritage”. In this policy, rutting is classified as acceptable vs. unacceptable depending on the environmental implications for each site. Any rutting in contact with or near streams and lakes is unacceptable (Berg et al., 2010).

This study compares several digitally derived soil wetness indices in terms of their conformance to actual wet-area conditions around streams and lakes. For references and recent developments pertaining to these indices, see Murphy et al. (2009, 2011), Tarboton (1997), Ma et al. (2010), Blöschl and Sivapalan, 1995). The areas for this case study are within the Krycklan catchment, Sweden (Fig. 1). The aim of this study is to develop a framework for mapping wet soils at high resolution, thereby improving the planning of forest operations, especially near streams and lakes.

2 Methods

2.1 Soil wetness transects

For the soil wetness survey we did not measure soil wetness but mapped indicators, along line transects on three areas within the well-studied Krycklan catchment (Laudon et al., 2013) (Fig. 1). The field survey was conducted 10–14 October 2011, during that period discharge measured at site C7 (Laudon et al., 2013) was 0.84 (Standard deviation, $SD = 0.13$) mm day^{-1} which matched the long term average 0.84 ($SD = 1.53$) mm day^{-1} for the period 1981–2013. In Area 1, eight 800–850 m transects were placed perpendicular to a number of ridges. This area is glaciated and till is dominating the soils, apart from a flat wetland located north east. The direction of the ice flow from northwest to southeast can be seen on the DEM in Fig. 3 by the orientation of the craig tails and drumlins. In Area 2, twelve transects were placed on a long ridge-to-valley hillslope. Till covers the hillslope, decreasing in thickness towards the top according to the Quaternary deposits map (1 : 100 000, Geological Survey of Sweden, Uppsala, Sweden). Area 2 also includes a mire at the bottom of the hill. In Area 3, eight 500 m transects were placed to cross the valley and floodplain of the Krycklan stream. The floodplain is filled with ice-river alluvium, containing mostly sand, gravel and boulders. The stream has cut down through the ice-river sediments forming ravines that become deeper towards the south. The upper east side of this valley is dominated by a moraine.

The geographical positions for each plot along the transect lines were determined using hand-held GPS, with an accuracy of < 10 m in 95 % of the measurements. Soil wetness was mapped according to the instructions for the Swedish Survey of Forest Soils (Anon, 2013). Temporal variations from dry to wet were to be ignored in favour of determining the underlying soil wetness regime and the related soil wetness classes, i.e., wet, moist, mesic-moist, mesic and dry soil, for full definitions see (<http://www-markinfo.slu.se/eng/soildes/fukt/skfukt1.html>). The process involved estimating the depth to the average water table level during the vegetation period, in reference to the elevation rise away from open water features (lakes, streams),

Title Page

Abstract

Introduction

Conclusions

References

Tables

Figures

◀

▶

◀

▶

Back

Close

Full Screen / Esc

Printer-friendly Version

Interactive Discussion



HESSD

11, 4103–4129, 2014

Evaluating digital terrain indices for soil wetness mapping

A. M. Ågren et al.

Title Page

Abstract

Introduction

Conclusions

References

Tables

Figures

◀

▶

◀

▶

Back

Close

Full Screen / Esc

Printer-friendly Version

Interactive Discussion

wetlands, ditches, and wet obligatory (hydric) vegetation. In short the five wetness classes were defined as: on *wet soils*, (i) there are frequent permanent water pools, (ii) one cannot walk dry-footed in low shoes; (iii) soils are organic (often fens); (iv) conifers occur only occasionally. On *moist soils*, (i) the groundwater table is on average at less than 1 m depth, (ii) one can walk dry-footed in low shoes, provided one can step on tussocks in the wetter parts; (iii) wetland mosses (e.g. *Sphagnum* sp.) dominate local depressions (pits), and trees often show a coarse root system above ground (germination point above soil); (iv) ditches are common; (v) soils range from organic (generally fens) to mineral (generally humus-podsols). On *mesic-moist soils*, (i) the groundwater table is also on average at less than 1 m depth, (ii) but one can walk dry-footed in low shoes over the entire vegetation area, except after heavy rain or snowmelt; (iii) areas with wetland mosses (e.g. *Sphagnum* sp., *Polytrichum commune*, *Polytrichastrum formosum*, *Polytrichastrum longisetum*) are common; (iv) trees show a coarse root system above ground (germination point above soil); (v) soils podsollic (humo-ferric to humic podsols); (vi) the mineral soil is covered by a thick peaty mor (thicker than on mesic soils). On *mesic soils*, (i) the groundwater table is on average at 1–2 m depth; (ii) one can walk dry-footed in low shoes over the area even after heavy rains/snowmelt; (iii) the bottom layer consists mainly of dryland mosses (e.g. *Pleurozium schreberi*, *Hylocomium splendens*, *Dicranum scoparium*); (iv) ferric podsols with a thin (4–10 cm) humus layer (mor) are common; (v) the bleached horizon is grey-white and well delineated against the rust-yellow, rust-red or brownish rust-red B horizon (the darker the colour, the wetter the soil). On *dry soils*, (i) the groundwater table is deeper than 1 m; (ii) dry soils are found on eskers, hills, marked crowns and ridge crests; (iii) the soils tend to be coarse in texture and include lithosol, boulder soil, and iron podsol formations, generally covered with a thin humus blanket on a thin bleached horizon; (iv) there can be significant bedrock exposure.

2.2 LiDAR acquisition and digital elevation model (DEM)

Since 2009, Lantmäteriet, the Swedish Mapping, Cadastral and Land Registration Authority, is generating high-resolution elevation scans using LiDAR technology (Light Detection and Ranging) for all of Sweden, with a point density of 0.5–1 points per m², an average *xy* point error of 0.4 m (SWEREF 99 TM), and a vertical accuracy of 0.1 m (RH 2000). The scanning of the study area was conducted during optimal conditions: after leaf fall and before snow cover, 11–14 October 2010. A 2 m × 2 m bare-ground Digital Elevation Model (or 2 m DEM for short), with an average elevation error of 0.5 m, was generated from the ground elevation returns of the LiDAR signals. This was done through triangulated irregular network (TIN) interpolation. The resulting DEM was hydrographically corrected by automatically breaching roadside impoundments and by removing DEM depression artifacts.

2.3 DEM processing

All DEM processing was done with ArcGIS 9.3 modeling tools and TauDEM 5.0. The 2 m DEM was used to derive the following terrain attributes in raster format: flow direction, aspect, curvature, plan curvature, cartographic depth-to-water (D_{TW}), flat areas, landform, puddles, toeslope, topographic position index (TPI) and topographic wetness index (TWI). These indices were evaluated at resolutions varying from 2 to 100 m.

Aspect was calculated on a 2, 4, 8, 16, 32 m resampled DEM, using bilinear interpolation. Since the aspect is given in degrees with both 0 and 360° facing north, aspect was computed in radians and then sine transformed to range from –1 to 1. *Curvature* was derived from the 2 m DEM in the direction of slope gradient (profile curvature) and perpendicular to the gradient (plan curvature). Profile curvature affects the acceleration and deceleration of flow while the plan curvature affects the convergence and divergence of the flow. Both curvature types were derived using windows spanning 3, 7 and 9 cells. A flatness index was derived from the 2 m DEM

HESSD

11, 4103–4129, 2014

Evaluating digital terrain indices for soil wetness mapping

A. M. Ågren et al.

Title Page

Abstract

Introduction

Conclusions

References

Tables

Figures

◀

▶

◀

▶

Back

Close

Full Screen / Esc

Printer-friendly Version

Interactive Discussion



HESSD

11, 4103–4129, 2014

Evaluating digital terrain indices for soil wetness mapping

A. M. Ågren et al.

Title Page

Abstract

Introduction

Conclusions

References

Tables

Figures

⏪

⏩

◀

▶

Back

Close

Full Screen / Esc

Printer-friendly Version

Interactive Discussion



using the zonal statistics function to determine the standard deviation of elevations within a radius of 10, 20, and 30 m. A low standard deviation indicates a flat area. *Puddles* within the DEM were identified by subtracting the 2 m DEM from a smoothed DEM, with smoothing referring to the mean elevations within a rectangle of 3×3 , 5×5 , 7×7 , and 9×9 cells. Negative differences locate local puddles. *Toe-slopes* were DEM-derived by creating a 0, 1 raster, with toe-slope cells marked as 1 and all other cells marked as 0. This was done twice by smoothing the 2×2 m DEM across 3×3 cells and 9×9 cells, and selecting those cells with a slope change of $11\text{--}20^\circ$. Topographic position index (TPI) compares the elevation of a cell to the mean elevation to the surrounding cells in a specified area. Positive values represent ridges and negative TPI values represent valleys while flat areas have a value near zero. TPI is scale dependent and was determined from the 2 m DEM using a cell moving window average of 17, 30, and 50 cells. Topographic landform classes (TLF) The TPI values were classified into 6 topographic landform classes (TLF) using the definition by (Weiss, 2001): 1 Ridge ($STDEV > 1$); 2 upper slope ($0.5 < STDEV \leq 1$); 3 middle slope ($-0.5 < STDEV < 0.5$, slope $> 5^\circ$); 4 flat slope ($-0.5 \leq STDEV \leq 0.5$, slope $\leq 5^\circ$); lower slopes ($-1.0 \leq STDEV < -0.5$); 6 valley ($STDEV < -1$). The numerically higher landform classes refer to lower slopes or valleys and would therefore be wetter than the numerically lower landform classes (ridges, upper slopes). Topographic wetness index (TWI) (Beven and Kirkby, 1979) was calculated using TauDEM 5.0.6. TWI was defined as: $TWI = \ln(a / \tan \beta)$ where a is the D_∞ specific catchment area (contributing area per unit contour length) and β is the D_∞ -slope, in radians (Tarboton, 1997). Flow in flat areas was calculated according to Garbrecht and Martz (1997). That means that a high TWI indicates areas where much water accumulates and the slope is low. In contrast, steep slopes drain water and are therefore drier as indicated by low TWI. Since estimating slope and therefore TWI is strongly scale dependent (Blöschl and Sivapalan, 1995), it was necessary to repeat the TWI derivation by smoothing the 2 m DEM using moving windows with 2, 4, 6, 10, 14, 24, 50, and 100 m diameters. Doing so generated 2, 4, 6, 10, 14, 24, 50, and 100 m spaced TWI grids, which were then

Evaluating digital terrain indices for soil wetness mapping

A. M. Ågren et al.

Title Page

Abstract

Introduction

Conclusions

References

Tables

Figures

◀

▶

◀

▶

Back

Close

Full Screen / Esc

Printer-friendly Version

Interactive Discussion



interpolated back to 2 m resolution by way of bilinear interpolation. Cartographic depth-to-water (D_{TW}) index calculates the depth (m) down to a modeled groundwater table throughout the landscape, in reference to zero depths at all locations where water is known or estimated to be at the surface. This index (Murphy et al., 2009, 2011) was derived from the 2 m DEM as follows: first the DEM was filled and the flow direction and flow accumulation data layers were generated using the D8 method (Jenson and Domingue, 1988; O’Callaghan and Mark, 1984). The resulting flow accumulation raster was used to derive the topographically defined flow channel networks with 0.5, 1, 2, 2.5, 4, 5, 8, 10, and 16 ha flow initiation thresholds. D_{TW} was then determined for each of the resulting flow networks by determining the least elevational differences between each DEM cell and its nearest stream cell according to the least-elevation path between these cells. Mathematically,

$$D_{TW} = \left[\sum \frac{dz_i}{dx_i} a \right] x_c \quad (1)$$

where dz/dx is the slope of a cell along the least-elevation path, i is a cell along the path, a is 1 when the path crosses the cell parallel to the cell boundaries and 1.414214 when it crosses diagonally; x_c represents the grid cell size (m).

2.4 Validation of terrain indices against field mapped soil wetness

2.4.1 Data preprocessing

Each variable was tested for normality using the Kolmogorov–Smirnow test (IBM SPSS Statistics 19). As a result, D_{TW} , TWI, TPI and flatness indices were log transformed to fit normality and to reduce the heteroscedasticity of model residuals. All index variables were scaled and centered using z scores (Eriksson et al., 2006a). Landform types were entered into the analyses as dummy variables.

2.4.2 Orthogonal projections to latent structures (OPLS)

The transect data for soil wetness were used to validate the digital terrain indices through direct point-by-point comparisons (of each $2\text{ m} \times 2\text{ m}$ cell). This was done using the multivariate statistical program SIMCA-P+ 12.0.1, Umetrics, Umeå. The statistical tests were done using the recently developed OPLS (orthogonal projections to latent structures) method (Eriksson et al., 2006a, b). This method, which is similar to principal component analysis, separates the variations of the predictors X (the DEM-derived soil wetness predictors) into two parts: one part that is predictive of Y (the field-determined soil wetness estimates), and one part that is orthogonal, i.e., not related to Y . In the loading plot, X variables with loadings that score high or low on the predictive axis are highly positively or negatively correlated to Y (Fig. 2). In SIMCA-P+, the program also calculates the influence of each X variable in the model, called variable importance in projection (VIP). Variables with large VIP, i.e., larger than 1, are the most relevant for explaining Y . In the OPLS loading plots of Fig. 2, variables with $\text{VIP} > 1$ and < 1 are marked by black and grey text, respectively.

2.4.3 Confusion matrix

The overall conformance of $D_{\text{TW}} \leq 1\text{ m}$ relative to the wet and moist soils within Areas 1, 2 and 3 was further tested by way of a confusion matrix. This was done by way of 4 D_{TW} performance groups: (i) True Positive (T_{P}) when the $D_{\text{TW}} \leq 1\text{ m}$ correctly identified a wet area; (ii) True Negative (T_{N}) when $D_{\text{TW}} > 1\text{ m}$ correctly identified a dry area; (iii) False Positive (F_{P}) or Type I error, i.e. when $D_{\text{TW}} \leq 1\text{ m}$ predicts wet soils when the soils are actually dry; (iv) False Negative (F_{N}), or type II error, i.e. $D_{\text{TW}} > 1\text{ m}$ predicts dry soils when the soils are actually wet. These tests were applied to the D_{TW} determinations as these vary by the D_{TW} -defining flow networks, using the flow-initiation thresholds from 0.5 to 16 ha. The accuracy (A_{CC}), or efficiency, of each of the $D_{\text{TW}} \leq 1$ or $> 1\text{ m}$

HESSD

11, 4103–4129, 2014

Evaluating digital terrain indices for soil wetness mapping

A. M. Ågren et al.

Title Page

Abstract

Introduction

Conclusions

References

Tables

Figures

◀

▶

◀

▶

Back

Close

Full Screen / Esc

Printer-friendly Version

Interactive Discussion



locations was assessed by way of:

$$A_{CC} = \frac{(T_P + T_N)}{(T_P + T_N + F_P + F_N)} \quad (2)$$

Also used was the Matthews correlation coefficient (M_{CC}) for which a value of 1 indicates a perfect fit, a 0 yields a results that is no better than random prediction, and -1 indicates a perfect negative correlation. M_{CC} was calculated as:

$$M_{CC} = \frac{T_P \times T_N - F_P \times F_N}{\sqrt{(T_P + F_P)(T_P + F_N)(T_N + F_P)(T_N + F_N)}} \quad (3)$$

Equations (2) and (3) were also used to determine the A_{CC} and M_{CC} values for the currently used 1 : 12 500 property map for Sweden in reference to the field determined soil wetness values. This map contains all officially recognized surface water and wetland features, including mires.

3 Results

The OPLS model generated models with high predictability (high R^2Y and Q^2) for soil wetness for Areas 1, 2 and 3 (Fig. 2). The two terrain indices that correlated best with the field-determined soil wetness data were TWI and D_{TW} . The effect of DEM resolution on the soil wetness predictor performance of these two indices can be seen from Fig. 2. Here, the D_{TW} values cluster closely together along the negative portion of the predictive soil wetness axis ($pq[1]$). In contrast, the scale-dispersed TWI values cut across the positive side of the horizontal axis, with TWI showing the strongest soil wetness prediction performance when derived from the 24 m (Area 1, Area 3) or 50 m (Area 2) DEMs. In particular, TWI calculated at 2 m resolution scored low on the predictive axis and high on the orthogonal axis ($p_o.s_o[1]$), thereby indicating that high resolution DEMs are not suitable for TWI based soil wetness determinations.

deviations of the A_{CC} and M_{CC} estimates by flow-initiation threshold: least for 1–2 ha for Areas 1 and 2, and least for 8–16 ha for Area 3. The somewhat decreasing A_{CC} and M_{CC} performance for D_{TW} using the flow-initiation threshold of 0.5 ha is likely due to two reasons: (i) extending the flow network to smaller and smaller reaches is directly limited by DEM resolution, (ii) with decreasing flow initiation, flow channels become drier for longer periods during each year.

Figure 5 illustrates differences between the wet areas of the Swedish property map and the D_{TW} maps: many small previously unmapped wet to moist areas along the transects conformed to the latter. Specifically, D_{TW} improved the M_{CC} for Area 1 (Table 1, Fig. 5). For Area 2, both maps produced similar A_{CC} and M_{CC} values, but the $D_{TW} < 1$ m criterion did not fully capture the extent of wetland below the long hillslope. To some extent, this can be remediated by extending the D_{TW} -based wetland delineations towards $D_{TW} > 1$ m. For Area 3, the transect across the valley, D_{TW} improved A_{CC} slightly, but improved M_{CC} strongly. Generally, M_{CC} is better measure of model performance than A_{CC} (Girard and Cohn, 2011).

4 Discussion

This study showed that the wet areas can be identified and mapped by way of DEM – derived data layers. The generally close agreement between the field-determined locations of wet soils and their corresponding TWI and D_{TW} values generally confirm the underlying assumptions that water movements across the study areas are driven by gravity and that topography controls the resulting water pathways. For the boreal forest landscape, these assumptions are generally consistent with delineating the enduring soil drainage and wetland distributions (Rodhe and Seibert, 1999).

For the TWI determinations, several methods of calculating flow accumulation exist, from the simple D8 algorithm (O’Callaghan and Mark, 1984) to the more complex MD ∞ (Seibert and McGlynn, 2007). Here, we used Tarboton’s D ∞ method (Tarboton, 1997) since Sørensen (2006) showed that this method gave the best results for predicting

HESSD

11, 4103–4129, 2014

Evaluating digital terrain indices for soil wetness mapping

A. M. Ågren et al.

Title Page

Abstract

Introduction

Conclusions

References

Tables

Figures

◀

▶

◀

▶

Back

Close

Full Screen / Esc

Printer-friendly Version

Interactive Discussion



Evaluating digital terrain indices for soil wetness mapping

A. M. Ågren et al.

Title Page

Abstract

Introduction

Conclusions

References

Tables

Figures

⏪

⏩

◀

▶

Back

Close

Full Screen / Esc

Printer-friendly Version

Interactive Discussion

soil wetness. Which particular TWI numbers indicate wet soils, however, vary by landscape, climate, and scale (Zinko et al., 2005; Western et al., 1999; Grabs et al., 2009; Güntner et al., 2004) The DEM scale is particularly problematic for the TWI-affecting slope derivation: with coarse DEM grids, flow channels and local depressions are not properly delineated; with fine DEM grids, local TWI variations are too strong to separate wetlands from uplands (Sørensen and Seibert, 2007). Figures 2 and 3 demonstrate that the scale as to which the TWI slope should be calculated depends on the landscape: in Area 1 and 3, the terrain was undulating and a 24 m DEM gave the best results. For Area 2, the 50 m DEM TWI derivation gave the best results along the hill slope. Since the best TWI derivations require DEM smoothing for all three areas (Fig. 3), TWI is not the best method for mapping small scale variations of wet areas along wetlands, streams and lakes.

In contrast to TWI, D_{TW} -based soil wetness mapping does not require DEM smoothing, and the amount of detail so revealed is mainly limited by DEM accuracy and resolution (Murphy et al., 2011, 2009, 2007). Figure 2 demonstrates that the D_{TW} -based wet area delineations are in fact less sensitive to the “scale” of the calculations and can therefore be considered a more robust method of predicting the wet soils. In this study the validation data set was recorded by studying the vegetation, which should reflect the average or median moisture condition of the site. By varying the flow initiation threshold, temporal variability of the stream network and adjacent wet soils can also be modelled, with lower and larger threshold values set for wet and dry seasons, respectively. For example, a 4 ha flow-initiation threshold was used to emulate end-of-summer flow and soil wetness, and soil drainage in general. Lowering this threshold to 1 and 0.25 ha would emulate soil wetness during wet summer weather and the snowmelt season (Murphy et al., 2011). D_{TW} maps based on 1–2 ha flow initiation thresholds were found to work best for (i) planning or locating road-stream channel crossings except for sandy landforms such as, e.g., floodplains and glacial outwash (Campbell et al., 2013), and (ii) for estimating the distribution of wet-area obligatory species (Hiltz et al., 2012; White et al., 2012).

maps in combination with D_{TW} as in Fig. 5 improves the high-resolution delineation of all the smaller wet areas next to streams and lakes.

It is suggested that the D_{TW} derived soil wetness maps can be used to reduce environmentally and economically costly off-road traffic surprises such as unacceptable rutting. For example, a recent D_{TW} advance dealt with mapping potential and actual soil disturbance impacts for the purpose of off-road soil trafficability assessment (Campbell et al., 2013). Additional forestry benefits refer to improving harvest scheduling (summer vs. fall vs. winter), in-field harvest navigation, selecting tree seedlings by species for planting dry vs. moist and wet sites, and optimizing block access routes and within block harvesting and wood forwarding trails (Arp, 2009). Elsewhere, D_{TW} -generated data layers proved useful in systematic wetland border delineations and wetland classification (Murphy et al., 2007; White et al., 2012). Similarly, D_{TW} derived maps could be useful to forecast upslope soil wetness once streams are blocked by, e.g., roads, trails, beaver dams, and logs falling across streams. In terms of vegetation indexing, Hiltz et al. (2011) was able to relate a plot-based indexing of vegetation by soil moisture regime preference to $\log_{10}(D_{TW})$. To that effect, Zinko et al. (2005) and Kunglerova et al. (2014) found a strong relationship between plant species richness, groundwater levels and local groundwater discharge areas.

5 Concluding remarks

D_{TW} and TWI are both good predictors of soil wetness. However, in terms of application across Sweden, best TWI soil wetness delineations are sensitive to scale and landscape variations, and are limited in providing soil wetness detail at less than the optimal resolution of 24 m. In contrast, D_{TW} is fairly scale-independent in predicting wet areas, and especially so at fine resolution. In addition, D_{TW} can be further optimized by accounting for landform and substrate permeability to achieve a consistent wet-area delineation accuracy of about $A_{CC} = 80\%$ and $M_{CC} = 0.40$. However, more research needs to be done to confirm this generalization, since till deposits, eskers and clay soils have different hydraulic conductivities. This affects the choice of setting the D_{TW}

HESSD

11, 4103–4129, 2014

Evaluating digital terrain indices for soil wetness mapping

A. M. Ågren et al.

Title Page

Abstract

Introduction

Conclusions

References

Tables

Figures

◀

▶

◀

▶

Back

Close

Full Screen / Esc

Printer-friendly Version

Interactive Discussion



determining threshold for stream-flow initiation in particular, and for water movement through watersheds in general. Selecting the optimal values for these thresholds by landform type would enable a systematical reduction of false positive and false negative wet-area determinations. In conclusion, D_{TW} maps have the potential to form the next generation of high resolution wet-area maps, and the process of doing that would find many applications pertaining to forest operations planning and elsewhere.

Acknowledgements. This study was funded by the Swedish Energy Agency, Mistra (Future Forest Project) Formas (ForWater project) and the STandUP for Energy program. The D_{TW} calculations were performed at the Forest Watershed Research Centre at the University of New Brunswick, Canada. Thanks to Bengt Olsson and Anders Larssolle for field data of soil moisture.

References

- Ahtiainen, M.: The effects of forest clear-cutting and scarification on the water-quality of small brooks, *Hydrobiologia*, 243, 465–473, doi:10.1007/Bf00007064, 1992.
- Aneblom, T. and Persson, G.: Studies of the variations in water-content in the unsaturated zone of an esker, *Nord. Hydrol.*, 10, 1–6, 1979.
- Anon: RIS – Riksinventeringen av skog, Fältinstruktion 2013, Department of Forest Resource Management and Department of Soil and Environment, Swedish University of Agricultural Science, Umeå, Uppsala, available at: <http://www-ris.slu.se/>, last access: 15 February 2014, 2013 (in Swedish).
- Arp, P. A.: High-resolution flow-channel and wet-areas maps: a tool for better forest operations planning, Sustainable Forest Management Network University of Alberta, Edmonton, AB, Canada, SFM Network Research Note, 55, 1–6, 2009.
- Berg, R., Bergkvist, I., Lindén, M., Lomander, A., Ring, E., and Simonsson, P.: Förslag till en gemensam policy angående körskador på skogsmark för svenskt skogsbruk, Arbetsrapport Nr 731, Uppsala, Skogforsk, 18 pp., 2010 (in Swedish).
- Beven, K. and Germann, P.: Macropores and water flow in soils revisited, *Water Resour. Res.*, 49, 3071–3092, doi:10.1002/Wrcr.20156, 2013.

Evaluating digital terrain indices for soil wetness mapping

A. M. Ågren et al.

Title Page

Abstract

Introduction

Conclusions

References

Tables

Figures

⏪

⏩

◀

▶

Back

Close

Full Screen / Esc

Printer-friendly Version

Interactive Discussion



HESSD

11, 4103–4129, 2014

Evaluating digital terrain indices for soil wetness mapping

A. M. Ågren et al.

[Title Page](#)[Abstract](#)[Introduction](#)[Conclusions](#)[References](#)[Tables](#)[Figures](#)[◀](#)[▶](#)[◀](#)[▶](#)[Back](#)[Close](#)[Full Screen / Esc](#)[Printer-friendly Version](#)[Interactive Discussion](#)

- Beven, K. J. and Kirkby, M. J.: A physically based, variable contributing area model of basin hydrology, *Hydrological Sciences Bulletin*, 24, 43–69, 1979.
- Bishop, K., Allan, C., Bringmark, L., Garcia, E., Hellsten, S., Högbom, L., Johansson, K., Lomander, A., Meili, M., Munthe, J., Nilsson, M., Porvari, P., Skyllberg, U., Sørensen, R., Zetterberg, T., and Åkerblom, S.: The effects of forestry on Hg bioaccumulation in nemoral/boreal waters and recommendations for good silvicultural practice, *Ambio*, 38, 373–380, 2009.
- Bishop, K., Seibert, J., Nyberg, L., and Rodhe, A.: Water storage in a till catchment, II: Implications of transmissivity feedback for flow paths and turnover times, *Hydrol. Process.*, 25, 3950–3959, doi:10.1002/Hyp.8355, 2011.
- Blöschl, G. and Sivapalan, M.: Scale issues in hydrological modelling: a review, *Hydrol. Process.*, 9, 251–290, doi:10.1002/hyp.3360090305, 1995.
- Burkhead, N. M. and Jelks, H. L.: Effects of suspended sediment on the reproductive success of the tricolor shiner, a crevice-spawning minnow, *T. Am. Fish. Soc.*, 130, 959–968, 2001.
- Buttle, J.: The effects of forest harvesting on forest hydrology and biogeochemistry, in: *Forest Hydrology and Biogeochemistry*, edited by: Levia, D. F., Carlyle-Moses, D., and Tanaka, T., Springer, Netherlands, 659–677, 2011.
- Campbell, D. M. H., White, B., and Arp, P. A.: Modeling and mapping soil resistance to penetration and rutting using LiDAR-derived digital elevation data, *J. Soil. Water Conserv.*, 68, 460–473, 2013.
- Eriksson, L., Johansson, E., Kettaneh-Wold, N., Trygg, J., Wikström, C., and Wold, S.: *Multi- and Megavariate Data Analysis, Part I Basic Principles and Applications*, Umetrics, Umeå, Sweden, 425 pp., 2006a.
- Eriksson, L., Johansson, E., Kettaneh-Wold, N., Trygg, J., Wikström, C., and Wold, S.: *Multi- and Megavariate Data Analysis, Part II Advanced Applications and Method Extensions*, Umetrics, Umeå, Sweden, 307 pp., 2006b.
- Garbrecht, J. and Martz, L. W.: The assignment of drainage direction over flat surfaces in raster digital elevation models, *J. Hydrol.*, 193, 204–213, 1997.
- Girard, J. M. and Cohn, J. F.: Criteria and metrics for thresholded AU detection, 2011 IEEE International Conference on Computer Vision Workshops (ICCV Workshops), 6–13 November 2011, 2191–2197, 2011.



Evaluating digital terrain indices for soil wetness mapping

A. M. Ågren et al.

Title Page

Abstract

Introduction

Conclusions

References

Tables

Figures

◀

▶

◀

▶

Back

Close

Full Screen / Esc

Printer-friendly Version

Interactive Discussion

Grabs, T., Seibert, J., Bishop, K., and Laudon, H.: Modeling spatial patterns of saturated areas: a comparison of the topographic wetness index and a dynamic distributed model, *J. Hydrol.*, 373, 15–23, doi:10.1016/j.jhydrol.2009.03.031, 2009.

Güntner, A., Seibert, J., and Uhlenbrook, S.: Modeling spatial patterns of saturated areas: an evaluation of different terrain indices, *Water Resour. Res.*, 40, W05114, doi:10.1029/2003wr002864, 2004.

Hiltz, D., Gould, J., White, B., Ogilvie, J., and Arp, P. A.: Modeling and mapping vegetation type by soil moisture regime across boreal landscapes, in: *Restoration and Reclamation of Boreal Ecosystems: Attaining Sustainable Development*, edited by: Vitt, D. H. and Bhatti, J. S., Cambridge University Press, Cambridge, 56–75, 2012.

Jenson, S. K. and Domingue, J. O.: Extracting topographic structure from digital elevation data for geographic information-system analysis, *photogramm. Eng. Rem. S.*, 54, 1593–1600, 1988.

Jutras, M.-F. and Arp, P. A.: Determination of hydraulic conductivity from soil characteristics and its application for modelling stream discharge in forest catchments, in: *Hydraulic Conductivity – Issues, Determination and Applications*, edited by: Elango, L., InTech, 189–202, doi:10.5772/20309, 2011.

Jutras, M.-F. and Arp, P. A.: Role of hydraulic conductivity uncertainties in modeling water flow through forest watersheds, in: *Hydraulic Conductivity*, edited by: da Silva, V. R., InTech, 33–54, doi:10.5772/3410, 2013.

Koch, K., Kemna, A., Irving, J., and Holliger, K.: Impact of changes in grain size and pore space on the hydraulic conductivity and spectral induced polarization response of sand, *Hydrol. Earth Syst. Sci.*, 15, 1785–1794, doi:10.5194/hess-15-1785-2011, 2011.

Kreutzweiser, D. P. and Capell, S. S.: Fine sediment deposition in streams after selective forest harvesting without riparian buffers, *Can. J. Forest Res.*, 31, 2134–2142, doi:10.1139/x01-155, 2001.

Kronberg, R.-M. The boreal journey of methyl mercury – from harvest to black alder swamps, Ph.D. thesis No 2014:II, Faculty of Forest Sciences, Swedish University of Agricultural Science, Umeå, 2014.

Kuglerova, L., Jansson, R., Ågren, A., Laudon, H., and Malm-Renöfält, B.: Groundwater discharge creates hotspots of riparian plant species richness in a boreal forest stream network, *Ecology*, 95, 715–725, doi:10.1890/13-0363.1, 2014.

Evaluating digital terrain indices for soil wetness mapping

A. M. Ågren et al.

Title Page

Abstract

Introduction

Conclusions

References

Tables

Figures

◀

▶

◀

▶

Back

Close

Full Screen / Esc

Printer-friendly Version

Interactive Discussion



Laudon, H., Hedtjärn, J., Schelker, J., Bishop, K., Sørensen, R., and Ågren, A.: Response of Dissolved Organic Carbon following Forest Harvesting in a Boreal Forest, *Ambio*, 38, 381–386, 2009.

Laudon, H., Taberman, I., Ågren, A., Futter, M., Ottosson-Löfvenius, M., and Bishop, K.: The Krycklan Catchment Study – a flagship infrastructure for hydrology, biogeochemistry and climate research in the boreal landscape, *Water Resour. Res.*, 49, 7154–7158, 2013.

Lemly, A. D.: Modification of benthic insect communities in polluted streams: combined effects of sedimentation and nutrient enrichment, *Hydrobiologia*, 87, 229–245, doi:10.1007/bf00007232, 1982.

Lisle, T. E.: Sediment transport and resulting deposition in spawning gravels, North Coastal California, *Water Resour. Res.*, 25, 1303–1319, 1989.

Ma, J. C., Lin, G. F., Chen, J. M., and Yang, L. P.: An improved topographic wetness index considering topographic position, 2010, 18th International Conference on Geoinformatics, 18–20 June 2010.

Munthe, J. and Hultberg, H.: Mercury and methylmercury in runoff from a forested catchment – concentrations, fluxes, and their response to manipulations, *Water Air Soil Poll.*, 4, 607–618, 2004.

Murphy, P. N. C., Ogilvie, J., Connor, K., and Arp, P. A.: Mapping wetlands: a comparison of two different approaches for New Brunswick, Canada, *Wetlands*, 27, 846–854, 2007.

Murphy, P. N. C., Ogilvie, J., and Arp, P.: Topographic modelling of soil moisture conditions: a comparison and verification of two models, *Eur. J. Soil Sci.*, 60, 94–109, 2009.

Murphy, P. N. C., Ogilvie, J., Meng, F. R., White, B., Bhatti, J. S., and Arp, P. A.: Modelling and mapping topographic variations in forest soils at high resolution: a case study, *Ecol. Model.*, 222, 2314–2332, 2011.

Nyberg, L.: Water-flow path interactions with soil hydraulic-properties in till soil at Gårdsjön, Sweden, *J. Hydrol.*, 170, 255–275, doi:10.1016/0022-1694(94)02667-Z, 1995.

Nyberg, L., Stähli, M., Mellander, P.-E., and Bishop, K. H.: Soil frost effects on soil water and runoff dynamics along a boreal forest transect: 1. Field investigations, *Hydrol. Process.*, 15, 909–926, doi:10.1002/hyp.256, 2001.

O’Callaghan, J. F. and Mark, D. M.: The extraction of drainage networks from digital elevation data, *Comput. Vision Graph.*, 28, 323–344, 1984.

Prevost, M., Plamondon, A. P., and Belleau, P.: Effects of drainage of a forested peatland on water quality and quantity, *J. Hydrol.*, 214, 130–143, 1999.

Evaluating digital terrain indices for soil wetness mapping

A. M. Ågren et al.

[Title Page](#)

[Abstract](#)

[Introduction](#)

[Conclusions](#)

[References](#)

[Tables](#)

[Figures](#)

[◀](#)

[▶](#)

[◀](#)

[▶](#)

[Back](#)

[Close](#)

[Full Screen / Esc](#)

[Printer-friendly Version](#)

[Interactive Discussion](#)



Rodhe, A. and Seibert, J.: Wetland occurrence in relation to topography: a test of topographic indices as moisture indicators, *Agr. Forest Meteorol.*, 98–9, 325–340, doi:10.1016/S0168-1923(99)00104-5, 1999.

Schelker, J., Eklöf, K., Bishop, K., and Laudon, H.: Effects of forestry operations on dissolved organic carbon concentrations and export in boreal first-order streams, *J. Geophys. Res.*, 117, G01011, doi:10.1029/2011jg001827, 2012.

Seibert, J. and McGlynn, B. L.: A new triangular multiple flow direction algorithm for computing upslope areas from gridded digital elevation models, *Water Resour. Res.*, 43, W04501, doi:10.1029/2006WR005128, 2007.

Seibert, J., Grabs, T., Köhler, S., Laudon, H., Winterdahl, M., and Bishop, K.: Linking soil- and stream-water chemistry based on a Riparian Flow-Concentration Integration Model, *Hydrol. Earth Syst. Sci.*, 13, 2287–2297, doi:10.5194/hess-13-2287-2009, 2009.

Sidle, R. C., Ziegler, A. D., Negishi, J. N., Nik, A. R., Siew, R., and Turkelboom, F.: Erosion processes in steep terrain – truths, myths, and uncertainties related to forest management in Southeast Asia, *Forest Ecol. Manag.*, 224, 199–225, 2006.

Soulsby, C., Youngson, A. F., Moir, H. J., and Malcolm, I. A.: Fine sediment influence on salmonid spawning habitat in a lowland agricultural stream: a preliminary assessment, *Sci. Total Environ.*, 265, 295–307, 2001.

Sørensen, R. and Seibert, J.: Effects of DEM resolution on the calculation of topographical indices: TWI and its components, *J. Hydrol.*, 347, 79–89, doi:10.1016/j.jhydrol.2007.09.001, 2007.

Sørensen, R., Zinko, U., and Seibert, J.: On the calculation of the topographic wetness index: evaluation of different methods based on field observations, *Hydrol. Earth Syst. Sci.*, 10, 101–112, doi:10.5194/hess-10-101-2006, 2006.

Tarboton, D. G.: A new method for the determination of flow directions and upslope areas in grid digital elevation models, *Water Resour. Res.*, 33, 309–319, 1997.

Western, A. W., Grayson, R. B., Bloschl, G., Willgoose, G. R., and McMahon, T. A.: Observed spatial organization of soil moisture and its relation to terrain indices, *Water Resour. Res.*, 35, 797–810, doi:10.1029/1998wr900065, 1999.

White, B., Ogilvie, J., Campbell, D. M. H., Hiltz, D., Gauthier, B., Chisholm, H. K., Wen, H. K., Murphy, P. N. C., and Arp, P. A.: Using the cartographic depth-to-water index to locate small streams and associated wet areas across landscapes, *Can. Water Resour. J.*, 37, 333–347, doi:10.4296/cwrj2011-909, 2012.

Zinko, U., Seibert, J., Dynesius, M., and Nilsson, C.: Plant species numbers predicted by a topography-based groundwater flow index, *Ecosystems*, 8, 430–441, doi:10.1007/s10021-003-0125-0, 2005.

HESSD

11, 4103–4129, 2014

Evaluating digital terrain indices for soil wetness mapping

A. M. Ågren et al.

Title Page

Abstract

Introduction

Conclusions

References

Tables

Figures

⏪

⏩

◀

▶

Back

Close

Full Screen / Esc

Printer-friendly Version

Interactive Discussion



Evaluating digital terrain indices for soil wetness mapping

A. M. Ågren et al.

Table 1. Accuracy (A_{CC} , %) and Matthews correlation coefficient (M_{CC}) calculated for Areas 1, 2 and 3 by D_{TW} determining flow-initiation threshold, also showing the averages and standard deviations across the areas and the flow-initiation thresholds. The best results are highlighted in bold. For comparison, numbers for the Swedish Property map (1 : 12 500) are also given.

		0.5 ha	1 ha	2 ha	2.5 ha	4 ha	5 ha	8 ha	10 ha	16 ha	Average	St. Dev.	Map (1 : 12 500)
A_{CC} (%)	Area 1	84.8	88.6	86.9	85.9	82	81.5	81.3	81.4	77.7	83.3	3.43	93.4
	Area 2	81.7	83.9	89.3	89.2	88.2	87.9	87.9	88.5	88	87.2	2.59	90.1
	Area 3	72.2	77.5	84.6	84.6	88.2	89	91.4	91.5	91.5	85.6	6.79	90.7
	St.Dev.	6.6	5.6	2.4	2.4	3.6	4.1	5.1	5.2	7.2	1.9	2.2	1.8
	Whole area	80.3	84.1	87.1	86.7	85.7	85.7	86.3	86.5	84.8	85.2	2.08	91.2
M_{CC}	Area 1	0.66	0.70	0.60	0.56	0.39	0.37	0.35	0.35	0.15	0.46	0.18	0.68
	Area 2	0.42	0.39	0.52	0.51	0.44	0.42	0.42	0.46	0.42	0.44	0.05	0.57
	Area 3	0.29	0.34	0.40	0.36	0.38	0.40	0.46	0.46	0.46	0.39	0.06	0.28
	St.Dev.	0.19	0.20	0.10	0.11	0.03	0.03	0.05	0.06	0.17	0.03	0.07	0.21
	Whole area	0.50	0.52	0.51	0.48	0.38	0.37	0.38	0.38	0.27	0.42	0.09	0.61

Title Page

Abstract

Introduction

Conclusions

References

Tables

Figures

⏪

⏩

◀

▶

Back

Close

Full Screen / Esc

Printer-friendly Version

Interactive Discussion



Evaluating digital terrain indices for soil wetness mapping

A. M. Ågren et al.

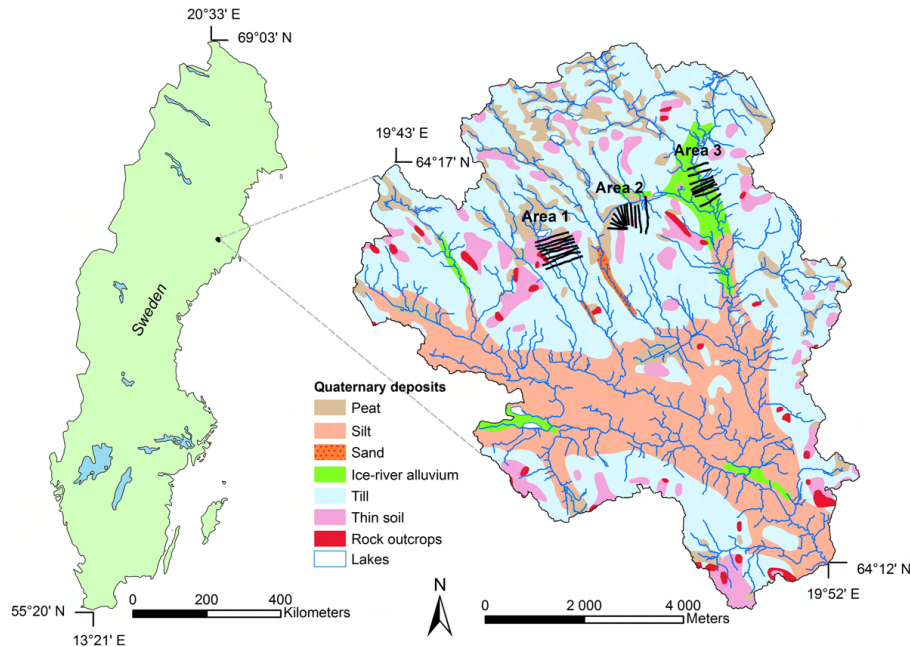


Fig. 1. Locator map for Areas 1, 2, and 3 with the Krycklan catchment with its quaternary deposits. The black lines show the location of the study transects.

[Title Page](#)[Abstract](#)[Introduction](#)[Conclusions](#)[References](#)[Tables](#)[Figures](#)[⏪](#)[⏩](#)[◀](#)[▶](#)[Back](#)[Close](#)[Full Screen / Esc](#)[Printer-friendly Version](#)[Interactive Discussion](#)

Evaluating digital terrain indices for soil wetness mapping

A. M. Ågren et al.

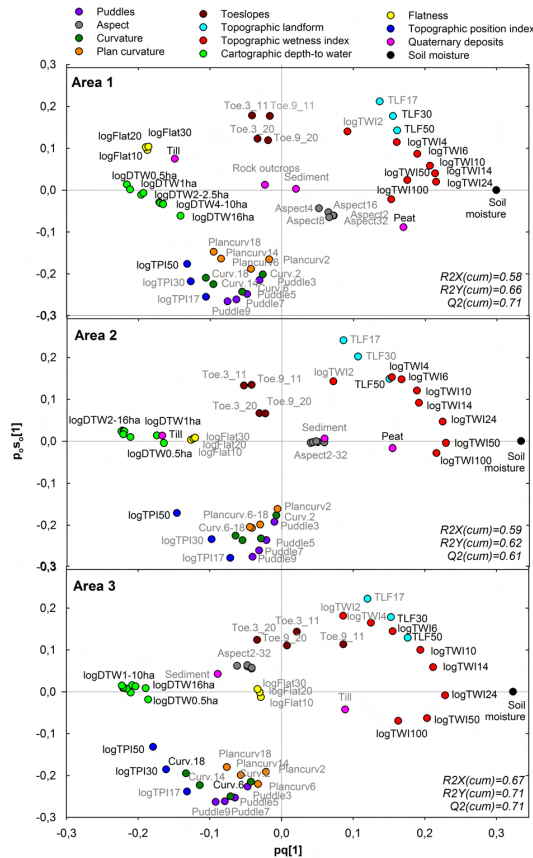


Fig. 2. OPLS loading plots for Area 1, 2 and 3 and their DEM-derived terrain indices regarding soil wetness prediction. $pq[1]$ is the predictive axis and $p_o_s_o [1]$ is the orthogonal (non-predictive) axis. Variables that have a high/low variable influence on the projection (VIP) are marked by black/grey text, respectively.

Title Page

Abstract

Introduction

Conclusions

References

Tables

Figures

⏪

⏩

⏴

⏵

Back

Close

Full Screen / Esc

Printer-friendly Version

Interactive Discussion



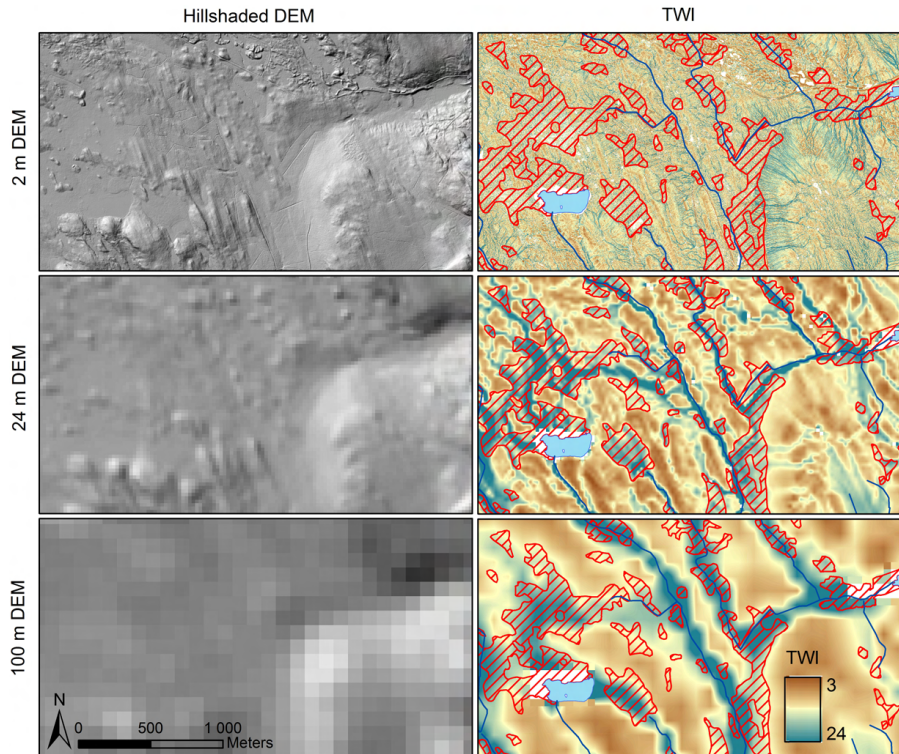


Fig. 3. The left panels show the hillshaded DEM in different resolutions. Topographic wetness index (TWI, right) derived from the 2, 24, and 100 m DEMs (left, hill-shaded), for a part of Area 1. Also shown on the right: lakes, streams and wetlands (crosshatched, red), previously mapped at 1 : 12 500.

Evaluating digital terrain indices for soil wetness mapping

A. M. Ågren et al.

Title Page

Abstract Introduction

Conclusions References

Tables Figures

◀ ▶

◀ ▶

Back Close

Full Screen / Esc

Printer-friendly Version

Interactive Discussion



Evaluating digital terrain indices for soil wetness mapping

A. M. Ågren et al.

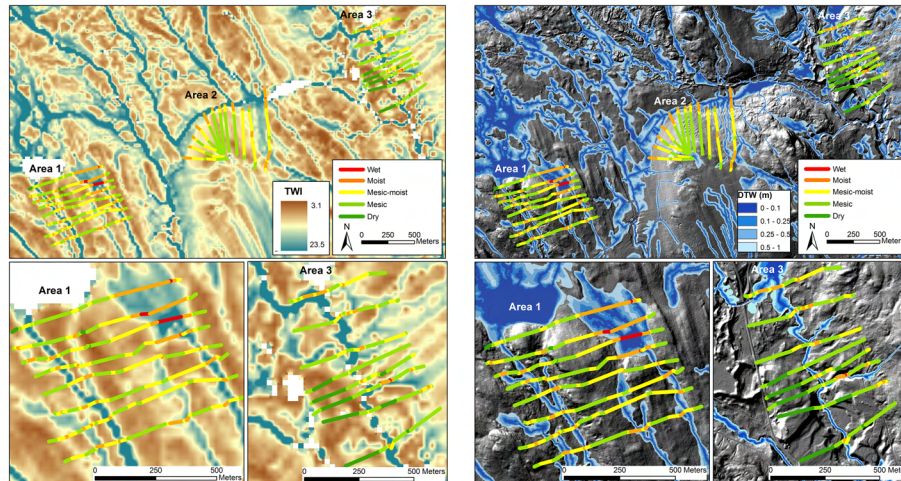


Fig. 4. Soil wetness transects (colored lines) for Areas 1, 2 and 3 on top of the 24 m DEM-derived TWI maps (left panel). The hill-shaded 2 m DEM is overlain by the cartographic depth-to-water (D_{TW}) classes ranging from 0 (dark blue) to 1 m (light blue), with flow channels mapped using a 1 ha flow initiation threshold (right panel). The lower panels show close-ups for Areas 1 (1 ha flow-initiation) and Area 3 (10 ha flow-initiation).

[Title Page](#)
[Abstract](#)
[Introduction](#)
[Conclusions](#)
[References](#)
[Tables](#)
[Figures](#)
[⏪](#)
[⏩](#)
[◀](#)
[▶](#)
[Back](#)
[Close](#)
[Full Screen / Esc](#)
[Printer-friendly Version](#)
[Interactive Discussion](#)


HESSD

11, 4103–4129, 2014

Evaluating digital terrain indices for soil wetness mapping

A. M. Ågren et al.

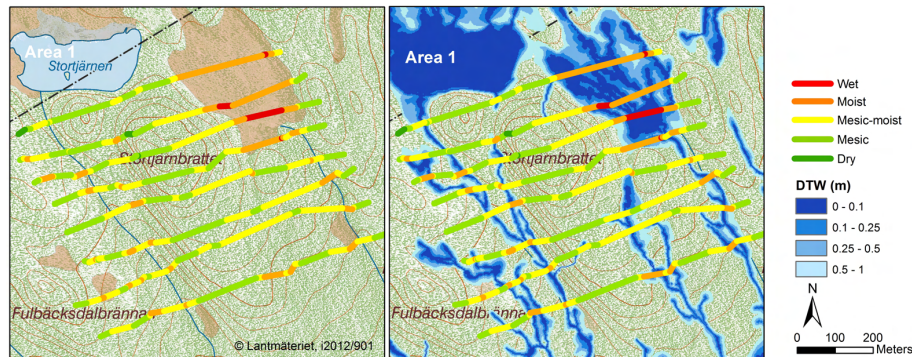


Fig. 5. Field-mapped soil wetness superimposed on today's most high resolution map (Property map 1 : 12 500). The wet areas of the Swedish Property Map are marked in beige (left) and are superimposed by the $D_{TW} < 1$ m map (right; 1 ha flow initiation).